TELKOMNIKA Telecommunication, Computing, Electronics and Control
Vol. 19, No. 2, April 2021, pp. 608~615
ISSN: 1693-6930, accredited First Grade by Kemenristekdikti, Decree No: 21/E/KPT/2018
DOI: 10.12928/TELKOMNIKA.v19i2.16519

The analysis of MF resin and $CaCO_3$ diffuser-loaded encapsulations to enhance the homogeneity of correlated color temperature for phosphor-converted LEDs

My Hanh Nguyen Thi[1], Phung Ton That[2]
[1]Faculty of Mechanical Engineering, Industrial University of Ho Chi Minh City, Vietnam
[2]Faculty of Electronics Technology, Industrial University of Ho Chi Minh City, Vietnam

Article Info

Article history:

Received Apr 27, 2020
Revised Aug 29, 2020
Accepted Sep 5, 2020

Keywords:

$CaCO_3$
Color uniformity
Luminous flux
MF resin
Mie-scattering theory
pc-LEDs

ABSTRACT

The most popular method used in the production of phosphor-converted LEDs (pc-LEDs) is dispensing phosphor freely. However, this method is inferior in generating good angular correlated color temperature (CCT) homogeneity. Thus, in this article, a diffuser-loaded encapsulation is proposed as a potential solution for better CCT uniformity. The paper provides a detailed investigation on how melamine formaldehyde (MF) resin and $CaCO_3$ loaded encapsulations impact the uniformity of CCT, as well as the lumen efficacy of pc-LEDs. The results demonstrate that between MF resin and $CaCO_3$ loaded encapsulations, the MF resin yields a higher light diffusion efficiency while the $CaCO_3$ maintains greater lumen efficacy. The photon scattering development is the key force behind the enhancement of the angular CCT uniformity in pc-LEDs' output when using the loaded encapsulations of MF resin and $CaCO_3$ particles. Since this package utilized mineral, it has reasonable cost and is quite easy to control while still being effective in enhancing the angular CCT homogeneity of pc-LEDs. Diffusers with 1% concentration of MF resin or 10% concentration of $CaCO_3$ are determined as an optimal solution for reducing the variance of angular CCT and increasing the lumen output.

Corresponding Author:

Phung Ton That
Faculty of Electronics Technology
Industrial University of Ho Chi Minh City
No. 12 Nguyen Van Bao Street, Ho Chi Minh City, Vietnam
Email: tonthatphung@iuh.edu.vn

1. INTRODUCTION

Encapsulation is one of the most favorable techniques used in pc-LED packaging as it helps to enhance the stability of LEDs in various working environments and improve the light extraction from the chip. An encapsulant consisting of mineral diffuser can result in the extraction efficacy with a high refractive index. Moreover, as the mineral diffuser greatly contributes to the increases of reflection, refraction, scattering of lights, and the uniformity of angular color temperature. Yet, when the refractive index of a mineral diffuser is too high, it is not advantageous to the high-quality pc-LED production due to the emitted lights cannot transmit through the contacted surface between the encapsulation layer and the air. In the process of producing LEDs, the extraction efficacy of light and the refractive index of the materials are two factors that needed to be focused with the latter being the more crucial one. In fact, the higher the index of refraction of the semiconductor material the more light emitted from the active zones of the LED chips are trapped. Moreover, when the disparity of the refractive index at the semiconductor-air interface is large, the total internal reflection occurs

and the performance of light extraction is notably degraded as a result. However, the encapsulation with a high index of refraction can enhance the light extraction efficacy from the high-refractive-index LED semiconductor chip. According to Snell's law, the light escape cone has a very small angle as the difference of refractive index at the semiconductor-air interface is high. GaN material for instance has the escape cone of only 23.50° and 4% photon escape probability [1]. For the unencapsulated AlGaInP, the escape cone is only 17° and as a result, the performance of light extraction is very low. Besides that, the light outside the escape cone will be absorbed if these light cannot escape from the semiconductor. Researchers put many efforts into increasing the amount of light transmitted from the semiconductors such as LED die geometric optimization [2] and surface roughening [3-6] but they have not successfully addressed the high contrast in refractive indices at the semiconductor-air interface yet. Lee and his team introduced an encapsulation structure consisting of several layers that are arranged in order of their refractive indices [7]. Particularly, the layer with the highest index of refraction is directly placed over the semiconductor chip while the low-refractive-index layers are considered as the outer ones. The result showed that this graded-refractive-index encapsulation can enhance the light extraction efficiency with a constant refractive index. As the encapsulation including mineral diffusers can get the lights reflected, refracted, and scattered, it can randomize the direction of propagation and make the far-field distribution isotropic. In addition, the mineral diffuser greatly contributes to the uniformity of the color distribution of multicolor devices. The mineral diffusers are designed with optically transparent or opaque materials, for example, TiO_2, CaF_2, SiO_2, $CaCO_3$, and $BaSO_4$; and their refractive indices and the encapsulation's are disparate [8]. The encapsulation of microparticles with high index of refraction (Titania, Magnesia, Yttria, Zirconia, Alumina, GaN, AlN, ZnO, ZnSe) that are embedded in a host matrix such as polymer does not cause the light to scatter if the distribution of the particles is uniform and their sizes are smaller than the wavelength [9]. According to the report of Gu's team, the light extraction performance is 1.85 times higher when the deposition of 520 nm diameter TiO_2 microsphere arrays is carried out onto the InGaN quantum wells (QWs) LED via the dipping method [10, 11]. Though TiO_2 has the refractive index of 2.5 in the visible band that agrees with that of GaN, it causes a large difference of the refractive index between the encapsulation film and the air, and thus, the encapsulation with high index of refraction is not the optimal solution. Meanwhile, the organic silicone powder results in weak effect of diffusion as its refractive index is similar to that of the encapsulated polymethylmethacrylate whose performance is inferior at high temperatures.

Besides the luminous flux, the other issue that needs focus is the color quality of the pc-LEDs. The phosphor particles are distributed randomly around the LED chip regardless of the LED chip emission is the main cause of the low color quality of pc-LEDs. The result of that random distribution is the inconsistency of the ratio in between the yellow light emitted from the phosphors and the blue lights from the LED chip, which occurs in all directions [12]. In the effort of enhancing the color quality, many methods were proposed consisting of conformal phosphor coating [13], electrophoretic deposition [14], evaporating solvent from a suspension of phosphor [15], and using luminescent ceramic plate [16]. These techniques aimed to simplify the process of producing phosphor encapsulation, reduce the differences of both correlated color temperature (CCT) and angular CCT distribution. However, they cannot solve the problem of color inhomogeneity as the distribution of phosphor grains does not take the stability of the yellow-blue light ratio into consideration [17]. To get the balance between the blue and yellow lights, the only factor that studies have focused on is the portion the yellow phosphor following the blue light direction [18]. In fact, the direction of blue lights is various and not only straight through the phosphor grains, as they are also absorbed, transmitted, and reflected by the phosphor particles in the LED package. Moreover, the light power that is absorbed by the phosphor includes the energy of heat which determined by the Stoke's shift, the nonradiated and radiated power (radiated power represents the emission spectrum). Thus, the layer containing phosphors can be used as a diffuser based on its influence on scattering. As the scale of phosphorus particle size changes from sub-micrometer to micrometer, the photon emission is enhanced owing to the effect of Mie scattering. However, being utilized as diffuser is just a side effect of phosphor particles and the main objective is to improve the angular color uniformity [19]. The silicone-encapsulated epoxy microspheres which is fabricated by blending heterogeneous liquid silicone were introduced by Kim's group to promote the LED color homogeneity [20]. Chen, together with his partners, reported the reduction of CCT variance from 1000 to 420 K with the angles ranging from −70° to 70° when ZrO_2 nanoparticles is added into silicone mixture that was dispersed on the phosphor film [21].

Acknowledging the problems above, our study proposes the diffuser-loaded encapsulation approach using melamine formaldehyde (MF) resin and $CaCO_3$, which has quite high refractive index, as the materials of loaded diffusers for heightening the CCT homogeneity and the efficiency of light output. The effects of these diffusers are investigated in accordance with their concentrations. The obtained results show that this method can greatly reduce the CCT variation, resulting in better color uniformity, and is beneficial to the control of high lumen efficiency.

2. SIMULATION AND COMPUTATION

2.1. MC-WLEDs simulation

There are two common methods to improve the refractive index of the materials. The first method is producing the polymer having the functional group with high index of refraction such as benzene ring or halogen through organic synthesis approach, and the second one is compounding high-refractive-index particles with encapsulation. For the second approach, the particles get their surfaces treated first, and are diffused homogeneously in the encapsulant afterwards. The agglomeration of microparticles occurs as the force of attraction between the microparticles is strengthened due to the high ratio of the surface to volume at a micrometer scale, which causes the optical scattering to be excessive. Thus, in the effort of achieving a high index of fraction for particle loaded encapsulation while minimizing the scattering and absorption loss, it is essential to attain the uniformity of dispersion process as well as the stabilization of microparticles. Our research applied the second method to experiments and used a procedure similar to Mont's group [21]. Initially, in order to prevent the particles from being reabsorbed by H_2O and affected by other contaminants, right after being dried, they are blended with toluene and stirred magnetically. Afterwards, surfactants with suitable amounts are added to the compound, and all of them are thrown into a mixture. In 2 hours, a reflux system is utilized to get the microparticles effectively coated with the surfactants. The point of using this refluxing method is to completely blend the microparticles and the surfactants together to avoid the agglomeration of these microparticles in the solution. The surface of microparticles are covered with a thin layer of surfactants that contributes to the interparticle forces modification, which results in better particle dispersibility. Dow Corning 6550 silicone gel is well mixed with the resultant surface-modified MF resin and $CaCO_3$ particles within 5 minutes by ultrasound bath. Finally, this gel mixture is applied in constructing pc-LED packages.

The physical model of a pc-LED used in our research experiments is illustrated in Figure 1 (a). In Figure 1 (b) is the list of technical parameters of this model. The last one, Figure 1 (c), is the diagram demonstrating the pc-LED simulation that is carried out with the application of a program named LightTools 8.1.0, and the Monte Carlo method. The pc-LED is constructed with a reflector, phosphor layers, and 9 LED chips. For the reflector, it has a bottom length of 8 mm, a surface length of 9.85 mm and a height of 2.07 mm. Each phosphor film of the LED has a thickness fixed at 0.08 mm with the size of phosphor particles of 14.5 μm average diameter. The LED chips are covered by the phosphor layers and embedded into the reflector. Each of them has the height of 0.15 mm, 1.14 mm^2 square base, and 1.16 W emission power at 453 nm peak wavelength.

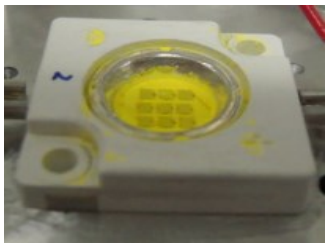

(a)

Lead frame: 4.7 mm Jentech Size-S
LED chip: V45H
Die attach: Sumitomo 1295SA
Gold Wire: 1.0 mil
Phosphor: ITC NYAG4_EL

(b)

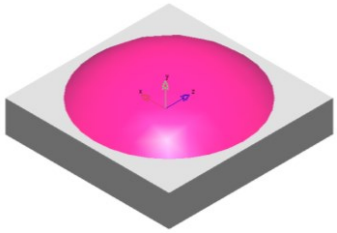

(c)

Figure 1. Illustration of phosphor-converted MCW-LEDs as doping $CaCO_3$: (a) the actual MCW-LEDs, (b) its parameters, (c) simulation of MCW-LEDs

2.2. Scattering computation

In this section, the results attained from using Mie theory [22, 23] and ray-tracing method [24, 25] are investigated and discussed in depth. The purpose is to utilize the Mie theory for more accurate optical characteristics' description of phosphor materials. The reason is that a large number of commercial optical software work based on Mie-scattering theory, for example Lighttools, Tracepro, and ASAP, and they normally process the phosphor scattering as Mie scattering to generate the optical simulation for pc-LED design. Moreover, as the Mie computation of the optical constants is modified, the optical simulation can be supported significantly and the performance of the software used for LED packaging simulation would be better. Based on Mie-scattering theorical demonstration, the expressions for computing the scattering coefficient $\mu_{sca}(\lambda)$, anisotropy factor $g(\lambda)$, and reduced scattering coefficient $\delta_{sca}(\lambda)$ might be demonstrated as:

$$\mu_{sca}(\lambda) = \int N(r) C_{sca}(\lambda, r) dr \quad (1)$$

$$g(\lambda) = 2\pi \int_{-1}^{1} \int p(\theta, \lambda, r) f(r) \cos\theta d \cos\theta dr \quad (2)$$

$$\delta_{sca} = \mu_{sca}(1-g) \quad (3)$$

In (1), *N(r)* is the diffusional particles' distribution density (mm^3) and C_{sca} indicates the scattering cross sections (mm^2). In (2), *p(θ,λ,r)* means the phase function, θ exhibits the scattering angle (°*C*), and *f(r)* indicates the size distribution function of the diffusor that the phosphorus film contains, and this parameter can be computed by expressions (4) and (5). Besides that, λ presents the light wavelength (nm), and r is known as radius of diffusional particles (μm).

$$f(r) = f_{dif}(r) + f_{phos}(r) \quad (4)$$

$$\begin{aligned} N(r) &= N_{dif}(r) + N_{phos}(r) \\ &= K_N \cdot [f_{dif}(r) + f_{phos}(r)] \end{aligned} \quad (5)$$

$N_{dif}(r)$ and $N_{phos}(r)$ included in *N(r)* are the diffusive and phosphor particles' densities, respectively. Meanwhile, $f_{dif}(r)$ indicates the size distribution function data of the diffusor and $f_{phos}(r)$ represents that of phosphor particles. Here, K_N indicates the diffusor unit quantity for one diffusor concentration. The computation of K_N can be carried out as:

$$c = K_N \int M(r) dr \quad (6)$$

M(r) here means the mass distribution of the diffusive unit, which is reckoned by the following expression:

$$M(r) = \frac{4}{3}\pi r^3 [\rho_{dif} f_{dif}(r) + \rho_{phos} f_{phos}(r)] \quad (7)$$

with $\rho_{diff}(r)$ symbolizes the diffusor density, and $\rho_{phos}(r)$ indicates the density of the phosphor crystal. The scattering cross sections C_{sca} in Mie-scattering theory could be:

$$C_{sca} = \frac{2\pi}{k^2} \sum_{0}^{\infty} (2n-1)(|a_n|^2 + |b_n|^2) \quad (8)$$

in which $k = 2\pi/\lambda$, a_n and b_n are expressed as follows:

$$a_n(x,m) = \frac{\psi_n'(mx)\psi_n(x) - \mathrm{m}\psi_n(mx)\psi_n'(x)}{\psi_n'(mx)\xi_n(x) - \mathrm{m}\psi_n(mx)\xi_n'(x)} \quad (9)$$

$$b_n(x,m) = \frac{m\psi_n'(mx)\psi_n(x) - \psi_n(mx)\psi_n'(x)}{m\psi_n'(mx)\xi_n(x) - \psi_n(mx)\xi_n'(x)} \quad (10)$$

with $x = k.r$, m presents the refractive index, $\psi_n(x)$ and $\xi_n(x)$ represent the Riccati - Bessel function. Thus, the diffusor's relative refractive index ($\mathrm{m_{dif}}$) can be: $m_{dif} = n_{dif} / n_{sil}$, and that of the phosphor ($\mathrm{m_{phos}}$) in the silicone is $m_{phos} = n_{phos} / n_{sil}$; after that, the phase function *p(θ,λ,r)* are calculated by:

$$p(\theta, \lambda, r) = \frac{4\pi\beta(\theta, \lambda, r)}{k^2 C_{sca}(\lambda, r)} \quad (11)$$

in which $\beta(\theta, \lambda, r)$, $S_1(\theta)$ and $S_2(\theta)$ indicate the angular scattering amplitudes whose computations can be expressed as:

$$\beta(\theta, \lambda, r) = \frac{1}{2}[|S_1(\theta)|^2 + |S_2(\theta)|^2] \quad (12)$$

$$S_1 = \sum_{n=1}^{\infty} \frac{2n+1}{n(n+1)} \begin{bmatrix} a_n(x,m)\pi_n(\cos\theta) \\ +b_n(x,m)\tau_n(\cos\theta) \end{bmatrix} \quad (13)$$

$$S_2 = \sum_{n=1}^{\infty} \frac{2n+1}{n(n+1)} \begin{bmatrix} a_n(x,m)\tau_n(\cos\theta) \\ +b_n(x,m)\pi_n(\cos\theta) \end{bmatrix} \quad (14)$$

The optical characteristics of YAG:Ce have been analyzed in many researches, but the fact that the factor α can change values at different Ce doping concentrations, crystal growth methods, and measurement equipment means YAG:Ce also needed to be studied in consideration of these situation . α usually varies in the range of 3–8mm^{-1} for the blue light. However, in terms of YAG:Ce optical ceramics comprised of small grains of crystal, the total light absorption is greater owing to the increase in internal reflections in the crystal grains, leading to the considerable improvement in light absorption; as a result, the range of α can be larger than 15 mm^{-1}. Assuming that the phosphor used in experiments is crystalline powder with high α, in this paper, the selection of the range for α variation is from 8 to 20mm^{-1} to study the changes of C_{sca} (453) for the blue light, and the reckoned results is presented in Figure 2. Figure 3 demonstrates the μ_{sca} which is computed by applying in (1). As Figure 2 illustrated, the scattering cross section is larger than the absorption cross section. This means the scattering impact of the phosphor material is very strong, which probably leads to higher blue-light absorption. Meanwhile, the absorption coefficient and scattering coefficient tend to increase along with the rise in the concentration of the phosphor particles. Thus, the color quality of WLEDs enhancement can be achieved with an appropriate amount of phosphor particles.

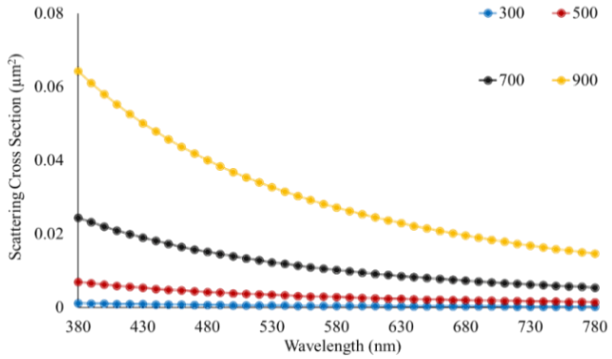

Figure 2. The scattering cross sections of $CaCO_3$ particles

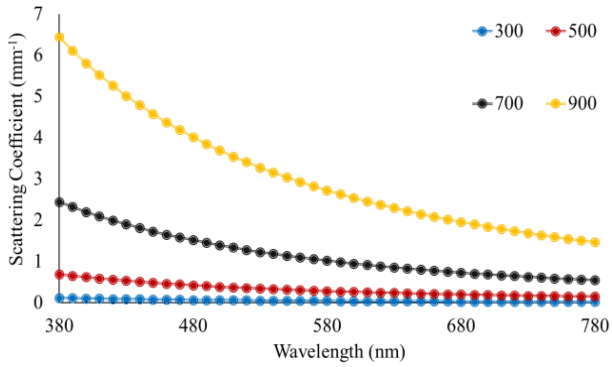

Figure 3. Scattering coefficients of $CaCO_3$ particles

As expressed in (3), the reduced scattering coefficient δ_{sca} is used to demonstrate the phosphorus scattering property, which helps to provide more thorough comparisons between the results from Mie theory and ray-tracing method, as illustrated in Figure 4. The final result of the optical constants for the phosphor particles can be accurately achieved by carrying out simulation with the ray-tracing method. Moreover, this

ray-tracing simulation gives the optical constants of YAG:Ce phosphor an evaluative estimation approach. Based on Figure 2 and Figure 4, obviously, the ray-tracing results in general present better μ_{sca} and δ_{sca} than the results from Mie theory do. Between the ray-tracing and Mie theoretical results, the ratios of μ_{abs} (453 nm) are usually around 1.47, while the ratios of μ_{abs} (555 nm) are approximately 1.63, for the blue lights.

The optic module of the optical measurement platform demonstrates that a pattern of Lambertian radiation is included in the blue or yellow lights emitted from the chips' surfaces, and the material used to fabricate the lenses and the support glass of for the phosphor slide is Schott BK7 glass. Besides that, the two integrating spheres have their inner surfaces covered by a diffuse white material whose absorption and scattering characteristics are 11.1% and 89.9%, respectively. Additionally, their inner surfaces play a role as receivers for collecting the lights that are transmitted and reflected. To produce the ray-tracing optical model, the Monte Carlo method is utilized, while the phosphor is used as a material for Mie-scattering theory. The Henyey–Greenstein phase function is utilized to measure the angular-scattering generation as the light scattering directions cannot be calculated directly by the ray tracing, and the results are demonstrated in Figure 5. At first, the original Mie theorical results are applied to the optical design, yet the ray-tracing results exhibits much better transmittance and lower blue light absorption, compared to that of the measurements results. The causes of these disparities are that in comparison with the real values, μ_{abs} and μ_{sca} are lower and $g(\lambda)$ is higher. Hence, to achieved more accurate optic constants, three mentioned methods were applied in the simulations. In this manner, they could stabilize one optical constant while simultaneously modify the other two constants to be closer to measurement results.

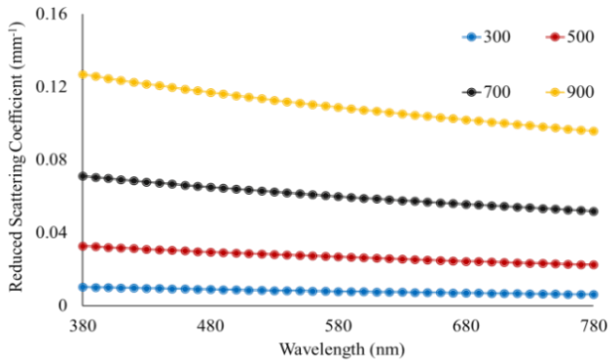

Figure 4. The reduced scattering coefficient of $CaCO_3$ particles

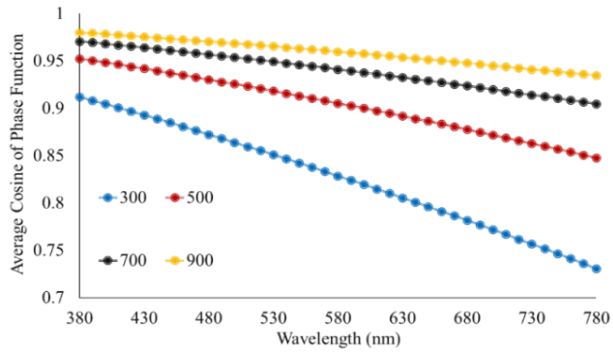

Figure 5. The phase function of $CaCO_3$ particles

3. RESULTS AND ANALYSIS

In Figure 6 is the angular CCT of pc-LED packaging with diffuser-loaded encapsulation of MF resin and $CaCO_3$. The experimented concentration of MF resin is from 1% to 10% while $CaCO_3$ concentration ranges from 0% to 50%. The angular CCT distribution of the light emitted from the phosphor layer is quite similar to the light emitted from the uncoated LED chip, and this phenomenon can be seen as Lambertian type. Specifically, the phosphor-emitted light has blue color at the center and becomes more yellowish when it comes near the edges. About the angle of CCT, the vertical direction at the central spot of the LED-chip surface is 0 degree, and the horizontal direction of the side of the LED chip is -90 or 90 degrees. Around 0 degree, the CCT is high but when it comes to -90 or 90 degrees, the CCT is low due to the difference between the angular

distributions of the blue light and the thickness of phosphor film. In general, as the distribution of angular CCT becomes greater, it leads to a large disparity between the max and min CCT. However, this CCT difference can be considerably degraded by using diffusers in LED packaging. At the same concentration, MF resin diffuser gives smaller spatial difference of CCT than $CaCO_3$ diffuser owing to the irregular characteristic of $CaCO_3$ diffuser. This is due to the scattering property of phosphor particles in $CaCO_3$ diffuser are not identical, and as a result, the spatial variance of CCT becomes larger. Figure 7 presents the change of luminous flux in pc-LED with MF resin and $CaCO_3$ diffusers. As can be seen from Figures 6 and 7, the spatial CCT difference and lumen output are inversely proportional to the concentration of the diffuser. In other words, the increase in diffuser content results in the decline of CCT variance and the luminous flux. However, the MF resin still has better value of angular CCT disparity reduction than $CaCO_3$ at all concentrations. Meanwhile, $CaCO_3$ diffuser shows greater effect in keeping the decrease of lumen efficacy stable, compared to that of the MF resin diffuser. At the similar concentration of 1%, the MF resin reduces angular CCT difference by 150% while $CaCO_3$ is approximately 70%. This is the result of unequal scattering effect of diffusers included in the encapsulation layer. In contrast, the decrease of lumen output is caused by the fact that the layer of phosphor and the chip in the encapsulation loaded with diffuser absorb the light from the LED chip. When taking scattering and light absorption properties into consideration, the diffuser is not beneficial to the lumen efficacy. Therefore, MF resin diffuser with 1% concentration is suitable to accomplish higher rate of reduced spatial CCT variance (more than 150%) and lower drop rate of luminous flux (below 15%). Nevertheless, when $CaCO_3$ diffuser with 10% concentration is added in the encapsulation layer, the decline in lumen output is smaller than that of diffuser with 1% MF resin due to the discrepancy in the loss of light scattering resulted from the diffuser integrated into the layer of encapsulation. Given that the MF resin and $CaCO_3$ have the same weight, the density and the particle sizes of MF resin are smaller than that of $CaCO_3$ (particle sizes of MF is 3 μm and of $CaCO_3$ is 15 μm). Moreover, the MF resin has much larger number of particles and stronger scattering than $CaCO_3$ particles. The increase in scattering is the cause of the reduction in the transmission of lights. In fact, it is necessary for these two factors to be balanced. Though the scattering improvement can enhance the CCT uniformity, the degradation of lumen efficacy will occur when the scattering events are excessive.

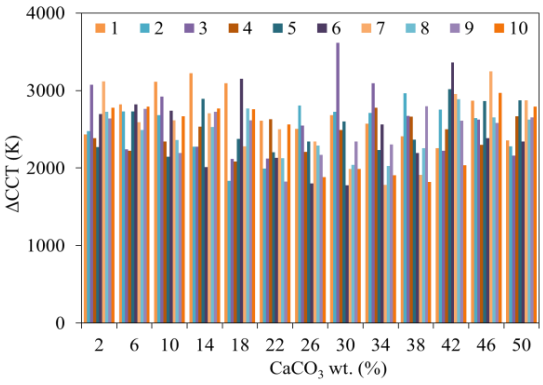

Figure 6. The ΔCCT of LED packaging with MF resin and $CaCO_3$ particles

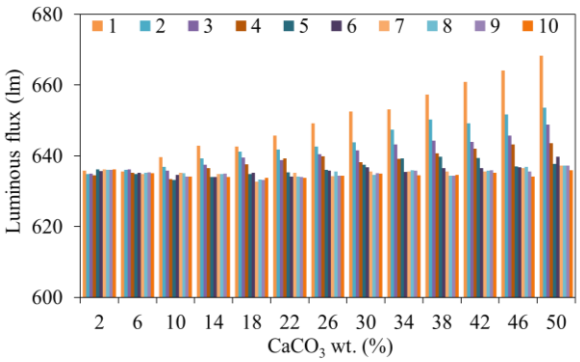

Figure 7. The luminous flux of LED packaging with MF resin and $CaCO_3$ particles

4. CONCLUSION

In summary, the investigation about the influences of diffusers, specifically the MF resin and $CaCO_3$ diffusers, on the pc-LED angular-dependent CCT homogeneity and luminous performance is demonstrated in this study. To construct the diffuser-loaded encapsulation for pc-LED packages, we also apply the method of dispersion in which the phosphor particle is freely dispersed. The reason to use this common method in packaging pc-LEDs with diffuser encapsulation is advantage and effectiveness in analyzing the impacts of this type of encapsulation on the reduction of spatial CCT difference and the decrease of lumen efficacy. The article presents that the diffusers have great effects on reducing the CCT variation, especially in package with MF resin diffuser. In other words, the diffusers can enhance the uniformity of CCT, which could be attributed to the increase of the photon scattering. Besides that, the increase of the diffuser concentration causes the decrease in both CCT difference and the lumen output. In addition, the results point out that the decrease of lumen output when using 1% MF resin diffuser is relatively similar to 10% $CaCO_3$ diffuser. The cause for these phenomena is the variation of the light scattering loss that occurs when mixing different diffuser in the encapsulation layer. The appropriate concentrations for diffusers to be used in encapsulation layer to achieve better CCT uniformity

and lumen efficiency are 1% of MF resin or 10% of $CaCO_3$. As the advantages of this diffuser packaging approach are cost efficiency and easy control, it is proven to be a more practical method for manufacturers to improve the color uniformity of pc-LEDs.

REFERENCES

[1] N. Anous, *et al.*, "Impact of blue filtering on effective modulation bandwidth and wide-angle operation in white LED-based VLC systems," *OSA Continuum,* vol. 1, no. 3, pp. 910-929, 2018.
[2] H. Y. Yu, *et al.*, "Solar spectrum matching with white OLED and monochromatic LEDs," *Appl. Opt,* vol. 57, no. 10, pp. 2659-2666, 2018.
[3] W. Zhong, *et al.*, "White LED light source radar system for multi-wavelength remote sensing measurement of atmospheric aerosols," *Appl. Opt,* vol. 58, no. 31, pp. 8542-8548, 2019.
[4] Z. Zhao, *et al.*, "Effective freeform TIR lens designed for LEDs with high angular color uniformity," *Appl. Opt,* vol. 57, pp. 4216-4221, 2018.
[5] H. L. Ke, *et al.*, "Lumen degradation analysis of LED lamps based on the subsystem isolation method," *Appl. Opt,* vol. 57, no. 15, pp. 849-854, 2018.
[6] Y. Zhou, *et al.*, "Comparison of nonlinear equalizers for high-speed visible light communication utilizing silicon substrate phosphorescent white LED," *Opt. Express,* vol. 28, no. 2, pp. 2302-2316, 2020.
[7] S. Sadeghi, *et al.*, "Quantum dot white LEDs with high luminous efficiency," *Optica*, vol. 5, no. 7, pp. 793-802, 2018.
[8] N. D. Q. Anh, *et al.*, "Selection of a Remote Phosphor Configuration to Enhance the Color Quality of White LEDs," *Curr. Opt. Photon,* vol. 3, no. 4, pp. 78-85, 2019.
[9] J. Hao, *et al.*, "Prediction of lifetime by lumen degradation and color shift for LED lamps, in a non-accelerated reliability test over 20,000 h," *Appl. Opt,* vol. 58, no. 7, pp. 1855-1861, 2019.
[10] S. Keshri, *et al.*, "Stacked volume holographic gratings for extending the operational wavelength range in LED and solar applications," *Appl. Opt,* vol. 59, no. 8, pp. 2569-2579, 2020.
[11] J. Ji, *et al.*, "Theoretical analysis of a white-light LED array based on a GaN nanorod structure," *Appl. Opt,* vol. 59, no. 8, pp. 2345-2351, 2020.
[12] Q. Xu, *et al.*, "Nanocrystal-filled polymer for improving angular color uniformity of phosphor-converted white LEDs," *Appl. Opt,* vol. 58, no. 27, pp. 7649-7654, 2019.
[13] C. Zhang, *et al.*, "Photometric optimization and comparison of hybrid white LEDs for mesopic road lighting," *Appl. Opt,* vol. 57, no. 16, pp. 4665-4671, 2018.
[14] T. L. Zhang, *et al.*, "Homo-epitaxial secondary growth of ZnO nanowire arrays for a UV-free warm white light-emitting diode application," *Appl. Opt,* vol. 59, no. 8, pp. 2498-2504, 2020.
[15] G. Zhang, *et al.*, "Spectral optimization of color temperature tunable white LEDs with red LEDs instead of phosphor for an excellent IES color fidelity index," *OSA Continuum*, vol. 2, no. 4, pp. 1056-1064, 2019.
[16] P. Zhu, *et al.*, "Spectral optimization of white light from hybrid metal halide perovskites," *OSA Continuum,* vol. 1, no. 6, pp. 1880-1888, 2019.
[17] X. P. Li, *et al.*, "Highly stable and tunable white luminescence from Ag-Eu3+ co-doped fluoroborate glass phosphors combined with violet LED," *Opt. Express,* vol. 26, no. 2, pp. 1870-1881, 2018.
[18] X. Bao, *et al.*, "User-centric quality of experience optimized resource allocation algorithm in VLC network with multi-color LED," *Opt. Express,* vol. 26, no. 21, pp. 27826-27841, 2018.
[19] F. B. Chen, *et al.*, "Investigation on Modulation Speed of Photon-Recycling White Light-Emitting Diodes With Vertical-Conduction Structure," *J. Lightwave Technol,* vol. 37, no. 4, pp. 1225-1230, 2019.
[20] H. S. E. Ghoroury, *et al.*, "Color temperature tunable white light based on monolithic color-tunable light emitting diodes," *Opt. Express,* vol. 28, no. 2, pp. 1206-1215, 2020.
[21] H. Lee, *et al.*, "Phosphor-in-glass with Nd-doped glass for a white LED with a wide color gamut," *Opt. Lett*, vol. 43, no. 4, pp. 627-630, 2018.
[22] Y. Tang, *et al.*, "Enhancement of luminous efficacy for LED lamps by introducing polyacrylonitrile electrospinning nanofiber film," *Opt. Express,* vol. 26, no. 21, pp. 27716-27725, 2018.
[23] W. Gao, *et al.*, "Color temperature tunable phosphor-coated white LEDs with excellent photometric and colorimetric performances," *Opt. Express,* vol. 57, no. 31, pp. 9322-9327, 2018.
[24] S. K. Abeysekera, *et al.*, "Impact of circadian tuning on the illuminance and color uniformity of a multichannel luminaire with spatially optimized LED placement," *Opt. Express,* vol. 28, no. 1, pp. 130-145, 2020.
[25] L. Xiao, *et al.*, "Spectral optimization of phosphor-coated white LED for road lighting based on the mesopic limited luminous efficacy and IES color fidelity index," *Appl. Opt,* vol. 57, no. 4, pp. 931-936, 2018.